Disclosure of some obscure mechanistic aspects of the copper-catalysed click reactions involving N_2 elimination promoted by the use of electron deficient azides from DFT perspective

Rooholah Roohzadeh, [†, ‡] Bahare Nasiri,[†, ‡] Antony Chipman,[§] Brian F. Yates,[§] and Alireza Ariafard*[,§]

[†]Department of Chemistry, Islamic Azad University, Central Tehran Branch, Shahrak Gharb, Tehran, Iran

[‡]Young Researchers and Elite Club, Central Tehran Branch, Islamic Azad University, Tehran, Iran

[§]School of Physical Science (Chemistry), University of Tasmania, Private Bag 75, Hobart TAS 7001, Australia. E-mail: alireza@utas.edu.au

ABSTRACT: We have used density functional theory to explore the copper(I)-catalysed reaction between a mesyl azide and a terminal alkyne that leads to a ketenimine whose interaction with nucleophilic water produces an amide. It is well reported in the literature that a cuprated triazole intermediate is formed during the course of such a catalytic cycle. In this contribution, we investigated the stability of this key intermediate by varying the R substituent on the azide and found that electron withdrawing R substituents make this intermediate more reactive toward ring opening/N_2 elimination; an electron withdrawing R substituent facilitates this process by weakening the N-N bond being cleaved. We also rationalised why the cycloaddition step in this class of click reaction is required to proceed via a binuclear mechanism. The copper(I) acetylide intermediate formed during the catalysis gains extra stability upon scavenging a second Cu complex, resulting in the cycloaddition step occurring with a lower activation barrier. We also noticed that, similar to the ring closure step, inclusion of a second Cu complex may accelerate the ring opening/N_2 elimination process. It was shown the ketenimine needs to coordinate to a copper centre via its nitrogen atom in order to be activated toward hydrolysis.

INTRODUCTION

Enormous interest is focussed on the experimental study of the copper(I)-catalysed cycloaddition of azides and terminal alkynes (CuAAC) to give triazoles,[1] due to the fact that the practical application of triazoles can encompass materials science, bioconjugation and drug discovery.[2,3,4] Many investigations propose that the catalytic cycle of CuAAC reactions should be initiated by π-coordination of the terminal alkyne to copper.[5] This coordination significantly increases the acidity of alkyne's hydrogen, promoting its deprotonation by an appropriate base, thereby producing copper(I) acetylide **I** and baseH$^+$ (Scheme 1).[6] This process is continued via addition of another copper to generate the binuclear complex **II**.[7] Addition of an azide to this binuclear complex affords cuprated triazole intermediate **IV**, preceded by the release of the second copper complex. Finally, **IV** is protonated by baseH$^+$, affording **V** and regenerating the copper catalyst.[8]

Scheme 1. Catalytic cycle proposed for the reaction of azides with terminal alkynes through CuAAC catalysis

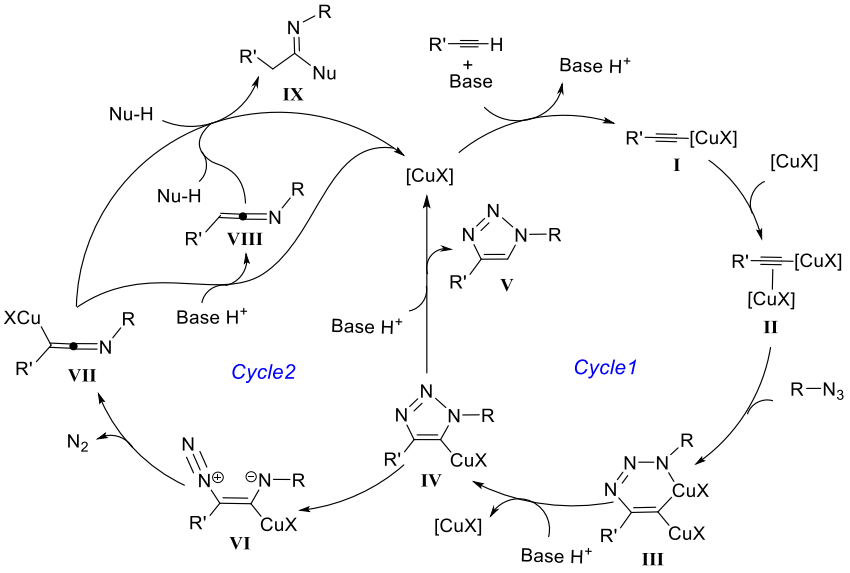

It should be noted that, for different substrates under specific conditions, products other than the triazole can be obtained.[9,10] For instance, when sulfonyl or phosphoryl azides are used, instead of formation of triazole (**V**), a N_2 molecule is liberated from the cuprated triazole intermediate **IV** and thus ketenimine **VIII** is obtained.[11] This result suggests that the identity of R substituent on an azide determines which product is preferentially achieved.[12] When R is of an electron donating character, triazole **V** is formed, whereas for electron withdrawing R substituents, N_2 elimination occurs and **VII** is produced.[7a] Eventually, addition of a nucleophile (Nu-H) to either **VII** or **VIII** forms product **IX** and leads to regeneration of the copper catalyst.

In the original report in this field, Chang et al. showed that amides are synthesized if a terminal alkyne, a sulfonyl azide, and water react with each other in the presence of CuI (eq 1). According to this experiment, water acts as the nucleophile (Nu-H).[13]

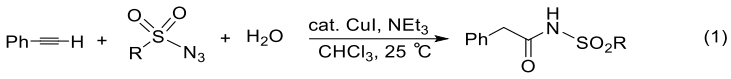

(1)

Electron withdrawing R-substituents are thought to decrease the stability of copper complex **IV**, which in turn facilitates N_2 elimination.[1e,7a] The first objective of this investigation is to address why this occurs. In other words, we want to better understand how the ring-opening rearrangement of cuprated triazole intermediate (**IV**) is promoted by electron withdrawing R substituents.

As illustrated in Scheme 1, the CuAAC reaction (cycle 1) was proposed to take place via a binuclear mechanism. Although this assertion has been proven for complexes with electron donating R groups, there is yet computational evidence to clearly show that this is also true for R groups with electron withdrawing character. In this study, we investigate a model CuAAC catalytic cycle with R = SO_2Me (methylsulfonyl/mesyl), with the aim of extending the scope of the explanation as to why, regardless of R identity, CuAAC reactions always prefer a binuclear mechanism and not a mononuclear one.

As discussed above, complex **IV** is a branching point for two competitive pathways. This complex can either stay on cycle 1 and react with $BaseH^+$ to give **V** or enter cycle 2 by undergoing a ring opening process followed by N_2 liberation. As discussed earlier, cycle 2 is expected to take place for electron withdrawing R groups. We will investigate these possibilities for R = mesyl and demonstrate that cycle 2 becomes favoured over cycle 1 when a second copper complex is incorporated into the N_2 elimination step.

At the end, by investigating the detailed mechanism for the reaction given in eq. 1, we intend to elucidate which intermediate (**VII** or **VIII**) is responsible for yielding product **IX** where water is considered as the nucleophile (Nu-H). We will indicate that intermediate **VIII** is far more reactive than **VII** albeit if it is activated by a copper catalyst.

RESULTS AND DISCUSSION

Effect of different R groups on the ease of ring opening/N_2 elimination. In the present study, a DFT-based analysis was carried out to investigate the effect of different R substituents with

various electronic properties (R = CH_3SO_2, CF_3, Ph, CH_3, *para*-NO_2-Ph, *para*-NH_2-Ph) on the reactivity of cuprated triazole intermediates toward ring opening/N_2 elimination. Table 1 summarizes our findings in this regard by considering CuI as the copper(I) catalyst. In accord with the previous studies,[11] the ring opening is anticipated to occur with the cleavage of the N^1-N^2 bond in cuprated triazole **A** via passing through transition structure $\mathbf{TS_{A\text{-}B}}$ (see the profile given above Table 1). The dinitrogen is subsequently evolved from **B** and then **C** is formed via $\mathbf{TS_{B\text{-}C}}$.

Table 1. Relative energy of different stationary points during the ring opening/N_2 elimination process based on the energy profile given below, the N^1-N^2 bond distance and second order perturbation energy between the lone pair on N^1 and the N^2-N^3 π^* orbital (E^2) in structure A

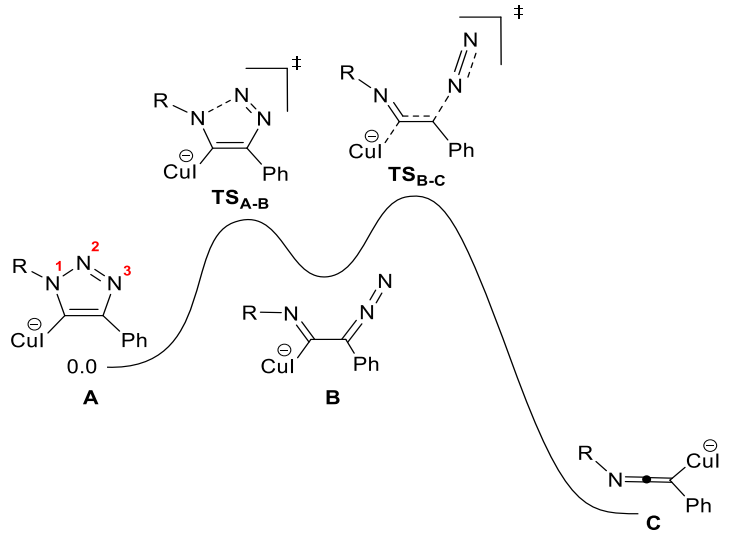

Entry	R	ΔG (kcal/mol)				N^1- N^2 (Å)	E^2 ($lp_{N1}\rightarrow\pi^*_{N2=N3}$)
		$\mathbf{TS_{A\text{-}B}}$	**B**	$\mathbf{TS_{B\text{-}C}}$	**C**	in **A**	kcal/mol
1	CH_3SO_2	12.9	9.3	17.3	-33.6	1.381	33.3
2	CF_3	13.9	11.7	20.1	-31.6	1.379	36.8
3	*para*-NO_2-Ph	19.8	18.3	24.4	-25.8	1.379	39.2
4	Ph	23.4	22.0	30.2	-23.0	1.372	42.2
5	*para*-NH_2-Ph	25.0	23.8	32.2	-21.7	1.372	43.1
6	CH_3	29.9	28.4	39.3	-17.1	1.360	46.3

Expectedly, the activation barrier to dinitrogen elimination increases as the R substituent becomes more electron donating. We found that, the stability of **B** relative to **A** is an important factor influencing the ease of the process; as the energy value of **B** increases, the energy values of transition structures $\mathbf{TS_{A\text{-}B}}$ and $\mathbf{TS_{B\text{-}C}}$ both increase. The above statement finds support from linear correlations between the energy values of **B** and $\mathbf{TS_{A\text{-}B}}$ (R^2 = 0.99) and of **B** and $\mathbf{TS_{B\text{-}C}}$ (R^2 = 0.97) (Figure S1 and S2, respectively). Indeed, a dinitrogen molecule is more easily evolved from complex **A** if the energy difference between **A** and **B** is small.

We claim that the stability of a triazole against ring opening is correlated with the N^1-N^2 bond nature. Table 1 lists the N^1-N^2 bond lengths for complex **A** with various R substituents. Results obtained from calculations indicate that the N^1-N^2 bond distances are shorter for electron donating R groups (e.g., CH_3) than for electron withdrawing ones (e.g., CH_3SO_2). To establish any possible correlation, we created a plot between the N^1-N^2 bond length and the relative energy of **B**. Interestingly, a good linear correlation (R^2 = 0.87) between those two variables was found (Figure S3), suggesting that the N^1-N^2 bond strength may have a significant effect on the stability of **A**. The natural bond orbital (NBO) analysis demonstrates that the second-order perturbation interaction between the N^1 lone pair (lp_{N1}) and $\pi^*_{N2=N3}$ in **A** is markedly increased if R is an electron donating group. Furthermore, a plot of the relative potential energy of **B** versus the interaction energy between lp_{N1} and $\pi^*_{N2=N3}$ gave a regression line with an R^2 value of 0.98 (Figure 1). According to these findings, it can be concluded that when R is of an electron donating character, the interaction between lp_{N1} and $\pi^*_{N2=N3}$ increases, thereby enhancing the contribution of the lower resonance structure given in Figure 1, resulting in strengthening of the N^1-N^2 bond and an enhanced resistance of complex **A** toward ring opening.

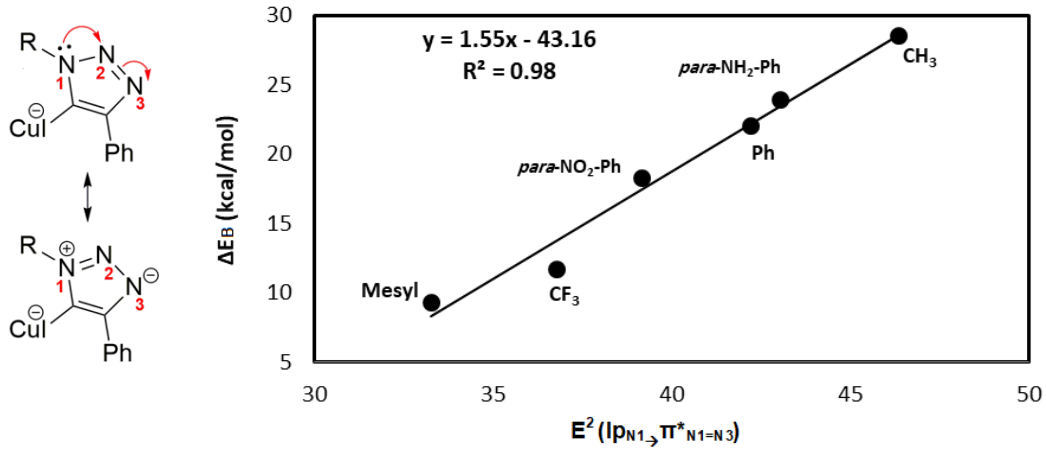

Figure 1. Plot of the potential energy of structure **B** (ΔE_B) versus the second order perturbation energy of interaction between lp_{N1} and $\pi^*_{N2=N3}$ in structure **A** for six different R substituents.

Mechanism of CuI-catalysed azide-alkyne cycloaddition where the R group is mesyl. We now focus our attention on the mechanism of Cu-catalysed azide-alkyne cycloaddition by considering R = mesyl as a representative of the electron withdrawing groups. Scheme 2 compares the stability of different copper adducts that may form by coordination of a substrate/base to CuI. According to this calculation, complex **2** was assigned as the most stable

adduct with a Gibbs free energy of -25.6 kcal/mol, leading us to set the energy of complex **2** as the reference point in our calculations.

Scheme 2. Relative energies (kcal/mol) of different adducts resultant from trapping of CuI by various reactants. The relative Gibbs and electronic energies (in parentheses) calculated at the B3LYP-D3BJ-CPCM/BS2//B3LYP-CPCM/BS1 level in chloroform are given in kcal/mol

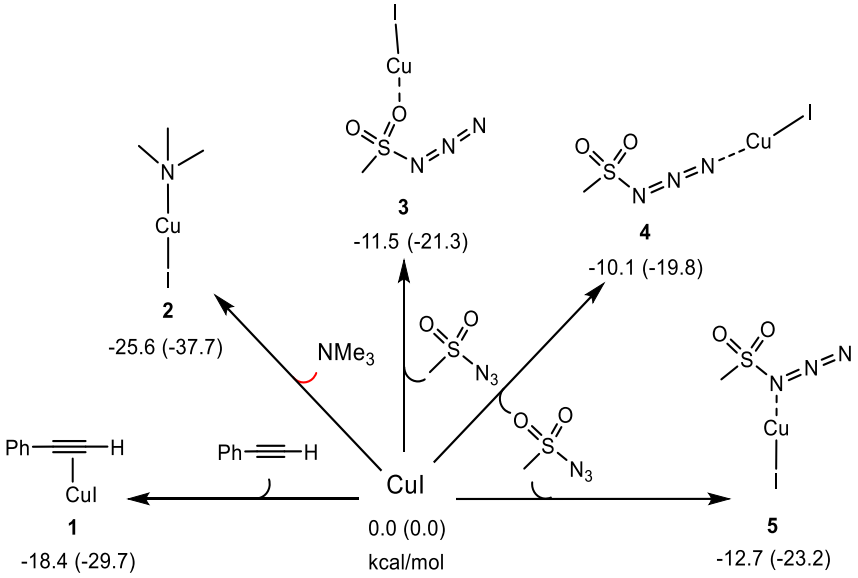

As outlined in Figure 2, the first step of the reaction is surmised to be coordination of a terminal alkyne to NMe_3CuI. This coordination leads to formation of three-coordinate intermediate **7** which lies 1.7 kcal/mol above the reference point. Liberation of NMe_3 from **7** via transition structure $\mathbf{TS_{7\text{-}8}}$ affords intermediate **8** in which NMe_3 is stabilized by a hydrogen bond with the terminal hydrogen of the coordinated alkyne. Subsequently, intermediate **9** is generated upon deprotonation of the terminal alkyne by NMe_3. The transformation **2** + **6** → **9** is calculated to be endergonic by 7.7 kcal/mol and requires an overall activation free energy of 14.2 kcal/mol.The endergonicity of this process mainly comes from the loss of amine binding energy. In other words, although NMe_3 serves as an appropriate base for deprotonation, it is also a strong coordinating ligand, rationalising why formation of the key acetylide complex **9** is an endergonic process. The outer sphere complex **9** is stabilized by the cation-anion interaction between NMe_3H^+ and $ICuCCPh^-$. The separation process **9** → $NMe_3H^+ + ICuCCPh^-$ is calculated to be endergonic by 22.4 kcal/mol, showing that the corresponding interaction is strong enough to force the NMe_3H^+ cation to remain in proximity to the anionic copper complex.[14]

In order for the alkynyl−azide cycloaddition to occur, the azide needs to be activated via its coordination to the copper centre. Our calculations show that the azide weakly interacts with the copper centre in **10** as evidenced by the endergonicity of the reaction **9** + $MeSO_2N_3$ → **10** (ΔG = 3.6 kcal/mol) and the long Cu-N^1 distance (3.338 Å). The low coordination ability of the azide mainly arises from the electron withdrawing character of the mesyl substituent which decreases the availability of the nitrogen (N^1) lone pair. Outer sphere complex **10** is expected to be in equilibrium with **11**, an intermediate which is a proper starting point for the cycloaddition process.

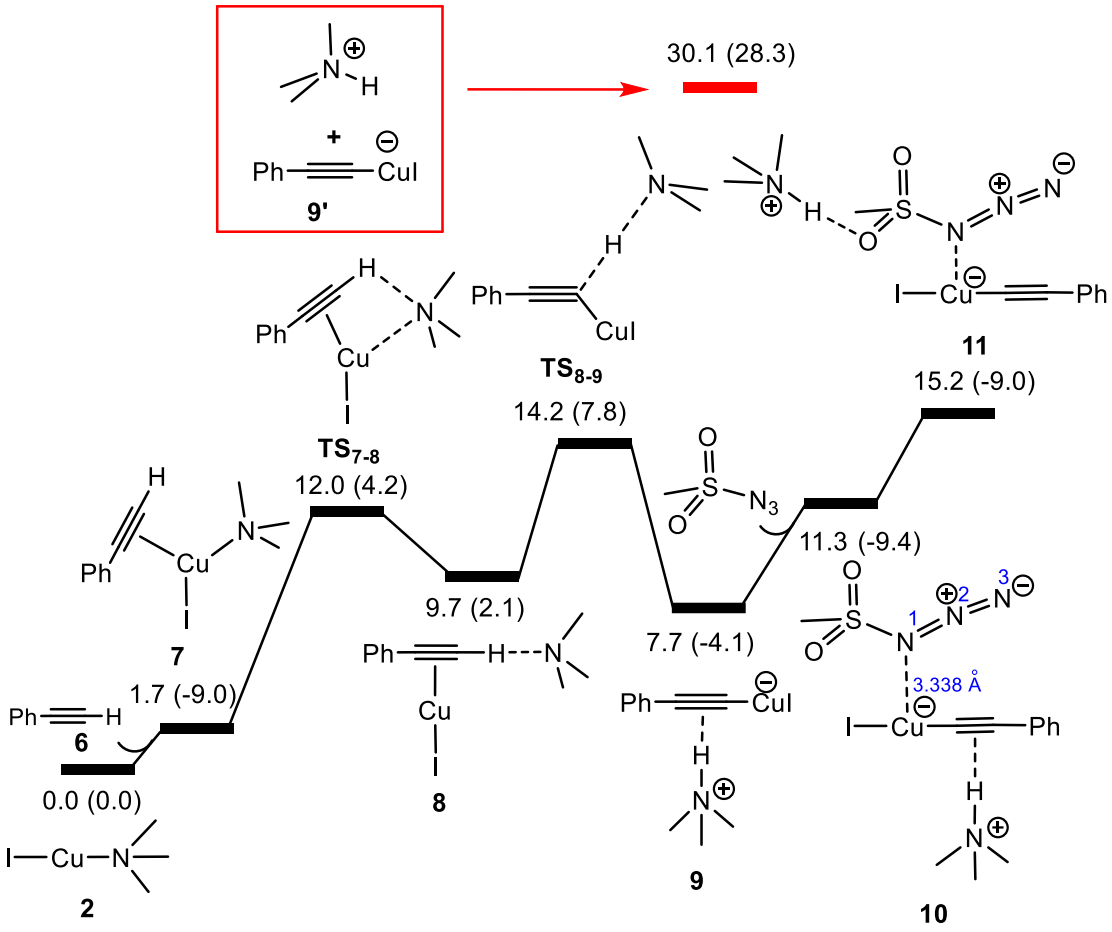

Figure 2. Calculated energy profile for formation of **11** starting from the resting state catalyst **2**. The relative Gibbs and electronic energies (in parentheses) calculated at the B3LYP-D3BJ-CPCM/BS2//B3LYP-CPCM/BS1 level in chloroform are given in kcal/mol.

The cycloaddition can occur through either a mononuclear or a binuclear pathway. Figure 3 compares the energy profile calculated for these alternatives. In the mononuclear pathway, the ring closure takes place via six-membered ring transition structure **TS11-12**. The IRC calculation revealed that, in contrast to previous studies,[11] this transition structure directly yields cuprated triazole **12** without any intermediate in between; efforts to locate **12′** were unsuccessful. The

overall barrier to cycloaddition via the mononuclear pathway is computed to be as high as 29.9 kcal/mol. This barrier seems too high to be accessible at room temperature. Thus, we anticipate that, in agreement with experimental observations, the operation of the mononuclear mechanism is improbable.

The binuclear mechanism initiates from coordination of a second copper complex to **11** via transition structure **TS11-13**. This coordination leads to formation of a *gem*-dicuprated complex **13** from which the cycloaddition takes place via transition structure **TS13-14** to give **14**. The resultant intermediate is highly reactive toward C-N coupling, forming **15** in a barrierless process. All attempts to obtain a transition structure connecting **14** to **12** were unsuccessful, a claim which is supported by a relaxed potential energy surface scan (Figure S4). The *gem*-dicuprated complex **15** is suggested to be in equilibrium with **12** via dissociation of the $ICuNMe_3$ complex. Starting from **13**, the binuclear pathway with an activation barrier of 15.4 kcal/mol is predicted to be 14.5 kcal/mol lower in energy than the mononuclear one (Figure 3).

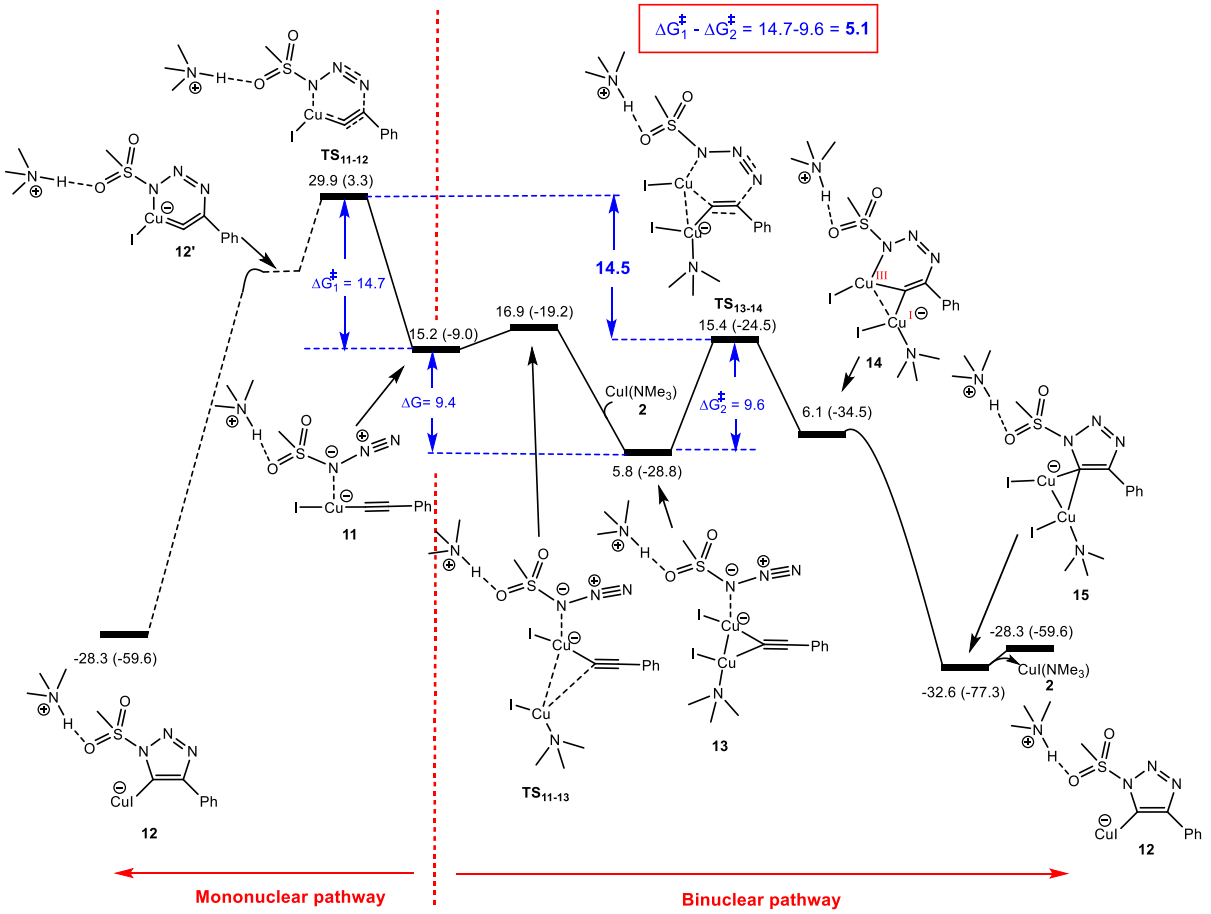

Figure 3. Calculated energy profile of mononuclear and binuclear pathways for azide–alkyne cycloaddition. The relative Gibbs and electronic energies (in parentheses) calculated at the B3LYP-D3BJ-CPCM/BS2//B3LYP-CPCM/BS1 level in chloroform are given in kcal/mol.

The favourability of the binuclear mechanism has been explained by two complimentary rationales as follows: (1) coordination of the second Cu complex reduces the ring strain in **TS$_{11\text{-}12}$** as compared with that in **TS$_{13\text{-}14}$**.[5b] (2) involvement of the second Cu-complex increases the stability of the nascent Cu(III) in **TS$_{13\text{-}14}$** by occupying its fourth coordination site.[5a] However, it becomes obvious from Figure 3 that the contribution of these two parameters to the energy difference between **TS$_{11\text{-}12}$** and **TS$_{13\text{-}14}$** (14.5 kcal/mol) is only $\Delta G^{\ddagger}_1 - \Delta G^{\ddagger}_2 = 5.1$ kcal/mol. Another critical contribution which has not been reported previously for this process,[15] is the high exergonicity of transformation **11** + CuI(NMe$_3$) → **13** ($\Delta G = -9.4$ kcal/mol). This result suggests that once the copper acetylide species is formed, it acts as a copper scavenger and immediately coordinates to another copper complex. The coordination of the second copper complex increases the stability of the key intermediate responsible for the cycloaddition step, resulting in the binuclear mechanism becoming highly favoured.

A competitive alternative for formation of **13** is coordination of CuI(NMe$_3$) to **8** followed by deprotonation and then coordination of mesyl azide. Our calculations for this alternative predict that the CuI(NMe$_3$) coordination with an overall activation energy of 13.2 kcal/mol should be the slowest step (Figure S5). Such a result suggests that **13** might be formed through this alternative without any necessity for the intermediary of the σ-acetylide complex **11**.

Mechanistic details of ring opening/N$_2$ elimination from the cuprated triazole intermediate. As shown in Figure 4, starting from cuprated triazole intermediate **12**, two distinct pathways are capable of competing with each other: (i) protodecupration and (ii) ring-opening/N$_2$ elimination.

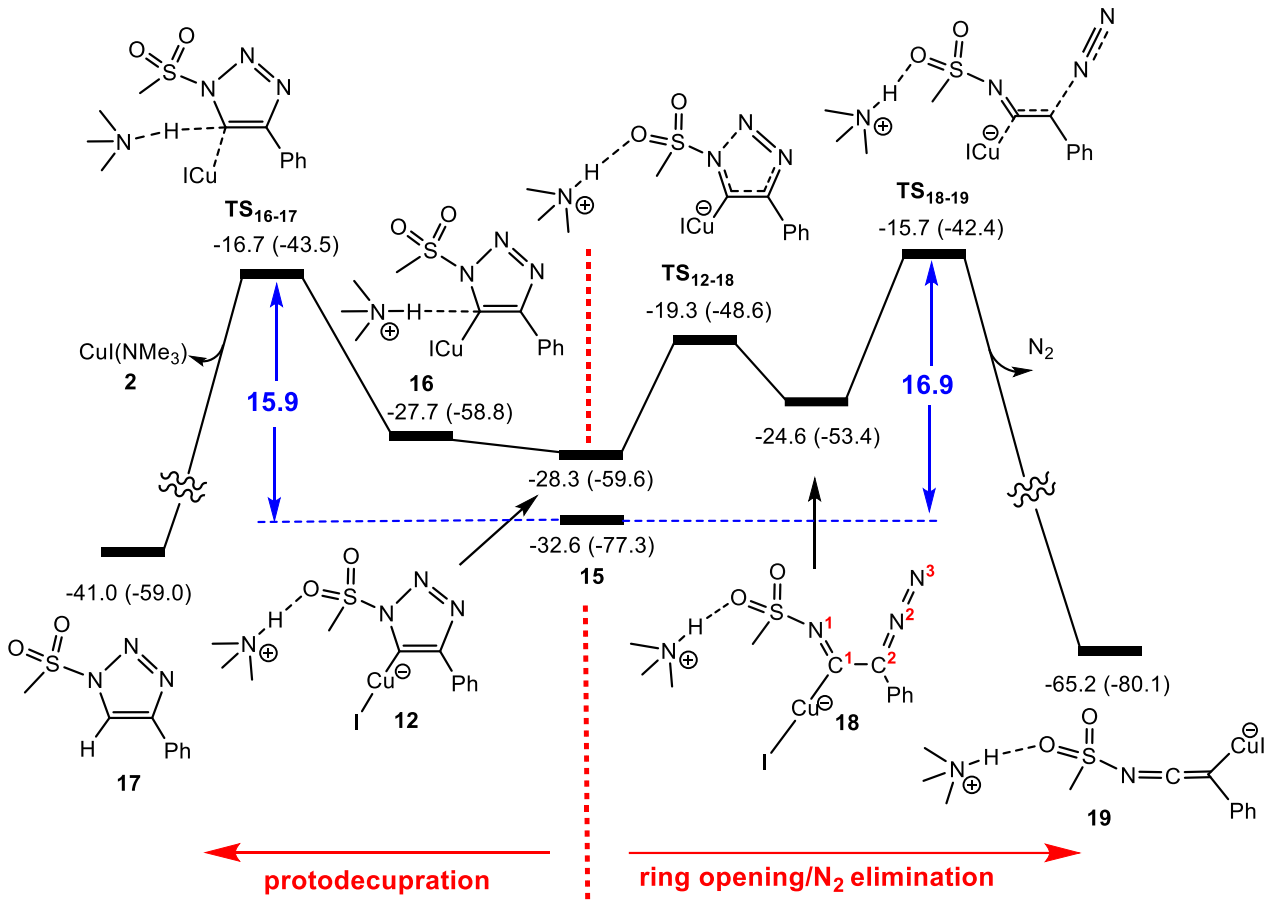

Figure 4. Calculated energy profile comparing protodecupration and ring opening/N_2 elimination precesses starting from cuprated triazole intermediate **12**. The relative Gibbs and electronic energies (in parentheses) calculated at the B3LYP-D3BJ-CPCM/BS2//B3LYP-CPCM/BS1 level in chloroform are given in kcal/mol.

Protodecupration is the pathway that gives triazole **17**. The overall activation barrier for this pathway is calculated to be 15.9 kcal/mol (Figure 4). The alternative pathway corresponds to ring-opening/N_2 elimination which has been previously discussed (see Table 1). It is apparent from Figure 4 that **TS18-19** is higher in energy than **TS12-18**. This is consistent with early theoretical studies, which suggest that the N_2 elimination step is more energy demanding than the ring-opening one.[11] However, in this section, we will show that this is not a correct statement.

Figure 4 shows that **TS16-17** lies 1.0 kcal/mol below **TS18-19** and so **12** is expected to preferentially involve in the protodecupration process. This is at odds with experimental observations that demonstrated the intermediacy of ketenimines in such a catalytic reaction.[1] In such a case, the N_2 elimination step possibly proceeds through an alternative mechanism with a lower energy barrier.

Interestingly, we found that similar to the cycloaddition reaction, if a second copper complex participates in the process, the N_2 elimination step accelerates. By that logic, intermediate **18** serves as a bidentate chelating ligand and binds to a CuI(NMe_3) complex through transition structure **$TS_{18\text{-}20}$** to give **20** in an exergonic fashion with ΔG = -3.0 kcal/mol (Figure 5). The ensuing intermediate is further activated toward N_2 elimination and undergoes it via **$TS_{20\text{-}21}$**. As a result, coordination of CuI(NMe_3) lowers the N_2 release barrier by 4.4 kcal/mol (see energy difference between $\Delta G_3^{\ddagger}$ and $\Delta G_4^{\ddagger}$ in Figure 5).

The bonding in these compounds (**20** and **18**) can be described in terms of a resonance hybrid between the two extreme structures **D** and **E** (Figure 6a). We should note that the ease of N_2 elimination depends on the contribution of form **E**. The elimination is triggered by the interaction of the Cu-C^1 σ orbital with the C^2-N^2 σ* orbital, as depicted in Figure 6a. Coordination of the second copper to **18** increases the contribution of **E**, causing the N_2 elimination to occur with a lower barrier. This claim is evident from shortening of the C^1-C^2 bond and lengthening of the C^1-N^1 and C^2-N^2 bonds upon moving from **18** to **20** (Figure 6b). The elongation of the C^1-N^1 and C^2-N^2 bonds in **20** can also be explained in terms of the distortion imposed by the Cu coordination.

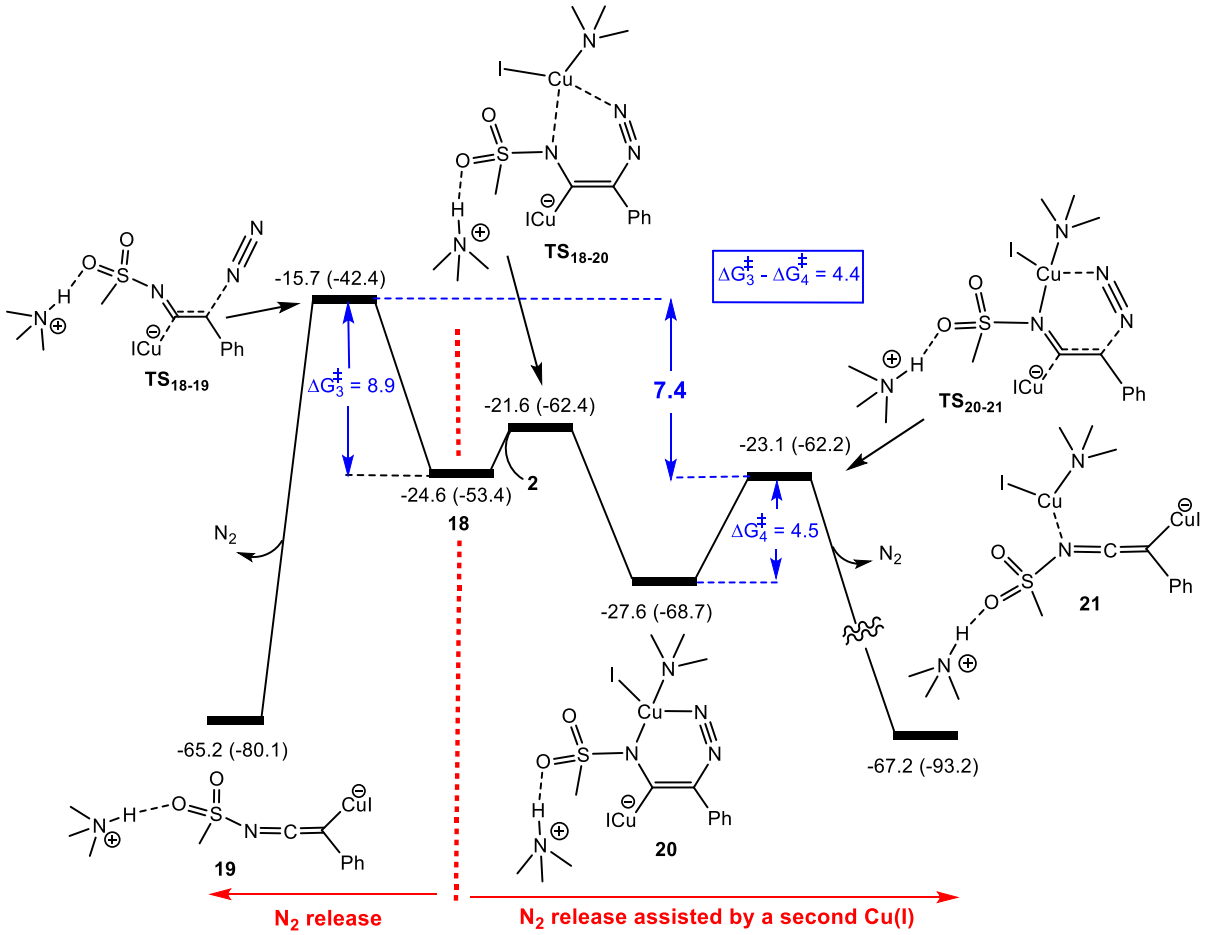

Figure 5. Calculated energy profile for N_2 elimination step, with and without using a second copper complex. The relative Gibbs and electronic energies (in parentheses) calculated at the B3LYP-D3BJ-CPCM/BS2//B3LYP-CPCM/BS1 level in chloroform are given in kcal/mol.

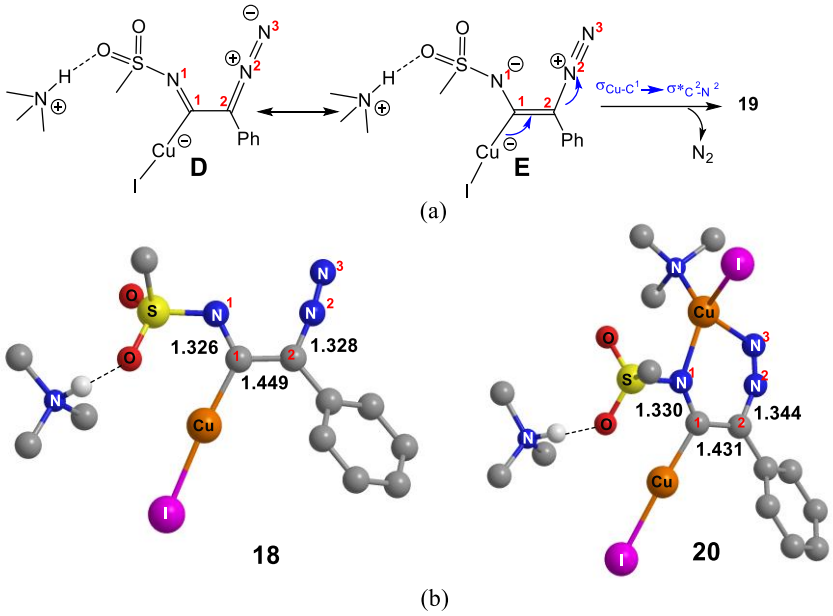

Figure 6. (a) Resonance hybrid for complex **18** described by two extreme structures **D** and **E**. (b) Optimized structures with selected structural parameters (bond lengths in angstroms) for **18** and **20** (H atoms omitted for clarity).

Plausible mechanism for reaction of water with the cuprated ketenimine intermediate. There are two conceivable pathways for the reaction of water with cuprated ketenimine **19**, as discussed in the introduction. Figure 7 compares the energy profiles for these two pathways where a water dimer was considered as the nucleophile. Pathway A (Brønsted acid activation mode) starts with isomerisation of **19** to **22** in which the ketenimine is activated toward water nucleophilic attack through hydrogen bonding between the ketenimine's nitrogen and NMe_3H^+. Subsequently, $(H_2O)_2$ attacks the internal carbon of the ketenimine via transition structure **TS$_{22\text{-}23'}$** and affords **23′**. The pathway B (Lewis acid activation mode), on the other hand, starts with a protodecupration process via **TS$_{19\text{-}23}$**. The resultant intermediate (**23**) then undergoes an isomerisation to a more stable species (**24**) in which the ketenimine is activated toward nucleophilic attack via coordination of the copper complex. The nucleophilic attack in this case leads to intermediate **25** via transition structure **TS$_{24\text{-}25}$**. It follows from Figure 7 that **TS$_{24\text{-}25}$** lies 11.9 kcal/mol lower in energy than **TS$_{22\text{-}23'}$** suggesting that the nucleophilic attack on the ketenimine is most likely to be accessed through Lewis acid activation.

The unfavourability of pathway **A** might be attributed to the presence of the Cu-C σ bond in the vicinal position to the carbon which is attacked by nucleophilic water. Indeed, the interaction of the Cu-C σ orbital with the N=C π* orbital in **22** increases the electron density in the p_z orbital of the internal carbon and therefore makes it less available to nucleophiles (Scheme 3). Our NBO calculations show that the second order perturbation energy for this orbital interaction ($\sigma_{Cu\text{-}C} \rightarrow \pi^*_{N=C}$) is very significant (67.5 kcal/mol).

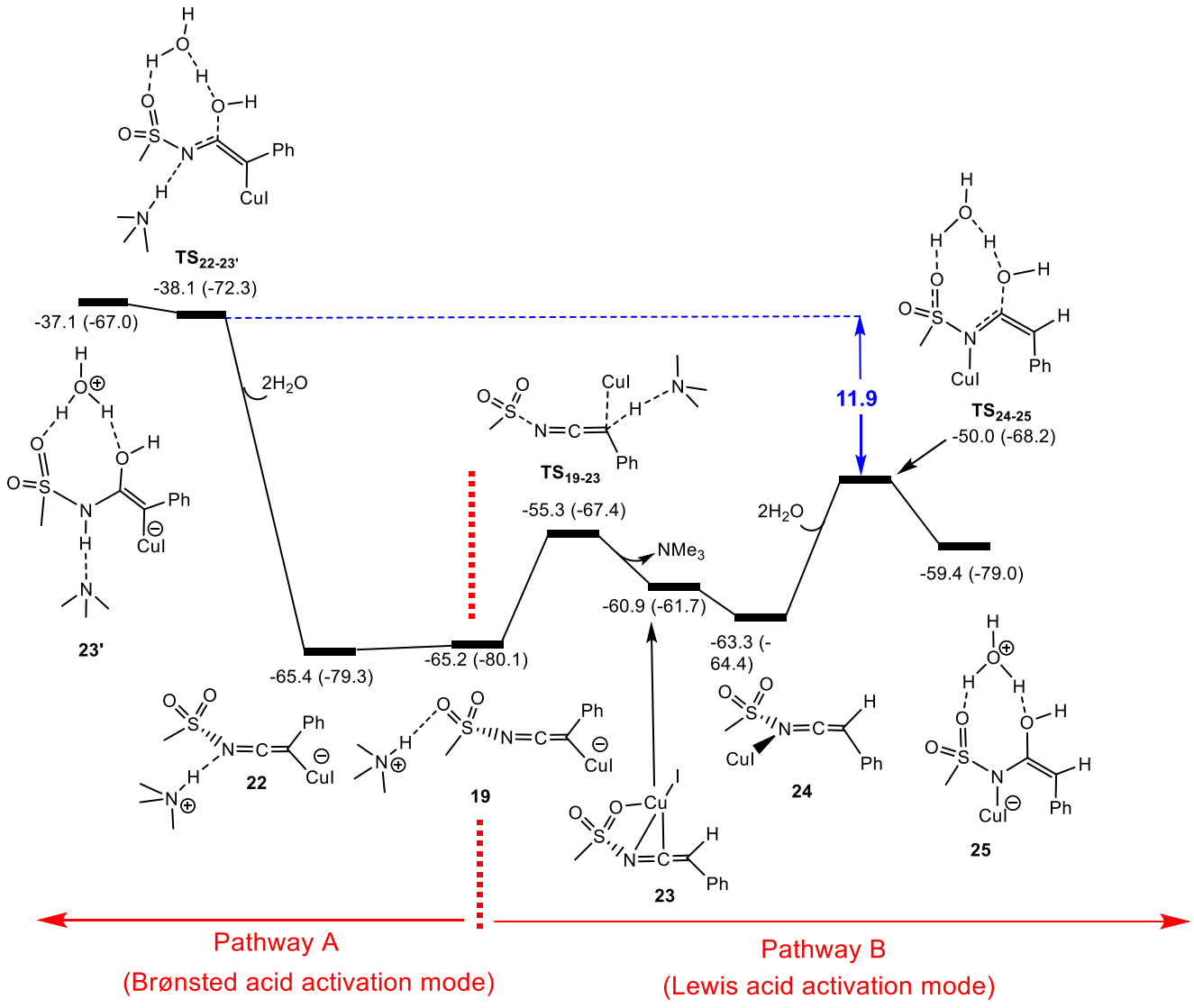

Figure 7. Calculated energy profile for the hydrolysis of **19** through two possible mechanisms. The relative Gibbs and electronic energies (in parentheses) calculated at the B3LYP-D3BJ-CPCM/BS2//B3LYP-CPCM/BS1 level in chloroform are given in kcal/mol.

Scheme 3. Interaction of the Cu-C σ orbital with the N=C π* orbital in 22

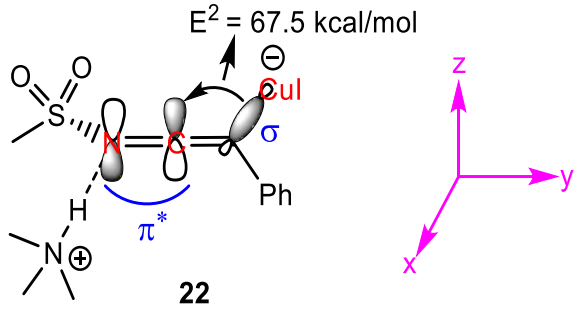

The energy profile outlined in Figure 8 shows how intermediate **25** is converted to final product (**prod**). The conversion starts with a proton transfer from H_3O^+ to the nitrogen atom by crossing transition structure **TS$_{25\text{-}26}$** to form the enol intermediate **26**. The required activation energy for this reaction is computed to be only 10.0 kcal/mol. The resulting enol intermediate gains further stability by tautomerising into a ketone form. We found that this tautomerisation is accelerated when a base (like NMe_3) is involved in the process. Addition of NMe_3 to **26** immediately gives ketone **27** in which a σ bond is formed between the copper and the substrate. Once NMe_3 deprotonates the O-H bond, the electrons in the C=C double bond of the enol **26** are polarized toward the C^{β} and stabilised by the copper complex. From intermediate **27**, the final product is formed via cleavage of the Cu-C(sp^3) bond through the proton transfer from NMe_3H^+ to the C^{β} with an activation energy of 11.0 kcal/mol.

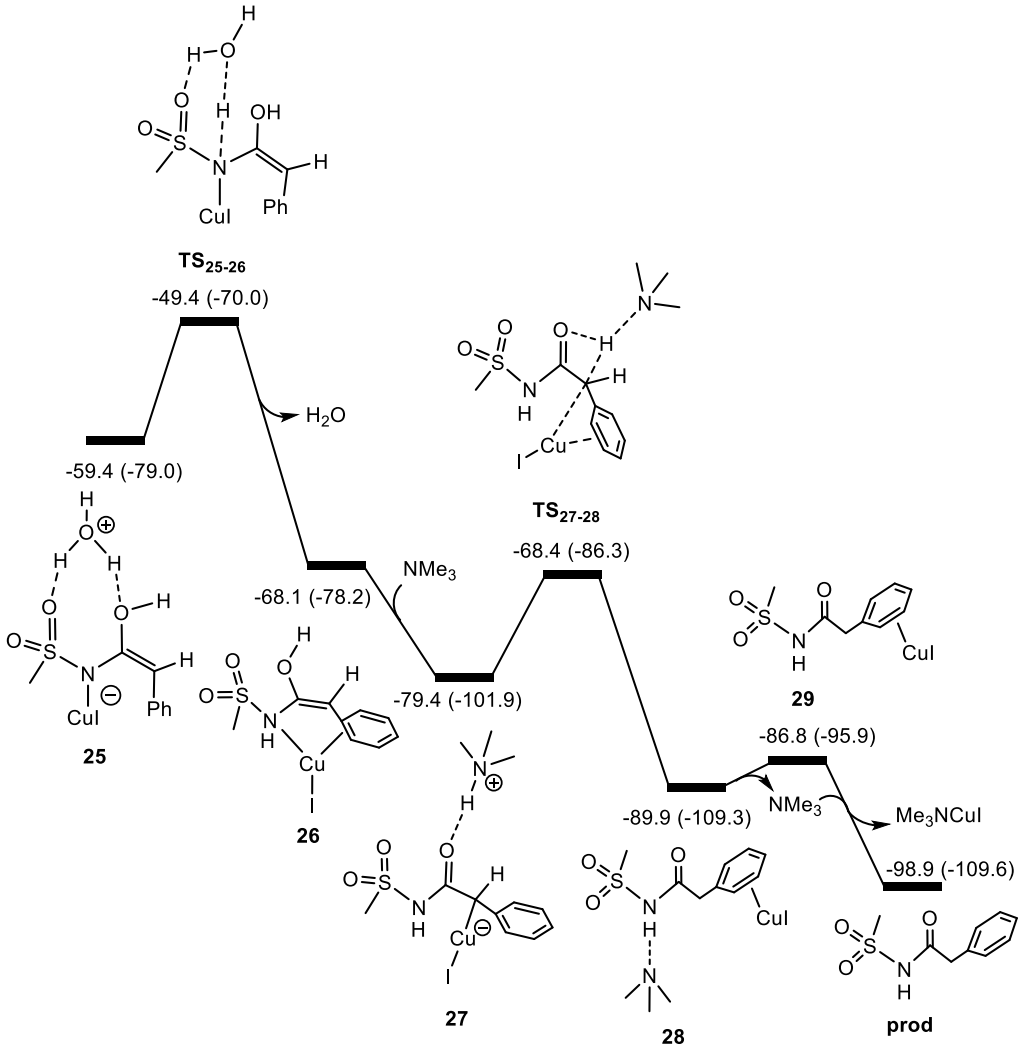

Figure 8. Calculated energy profile for conversion of intermediate **25** to final product. The relative Gibbs and electronic energies (in parentheses) calculated at the B3LYP-D3BJ-CPCM/BS2//B3LYP-CPCM/BS1 level in chloroform are given in kcal/mol.

Proposed mechanism derived from DFT calculation. A detailed catalytic cycle derived from DFT calculations for the Cu-catalysed click reaction between an electron deficient azide (mesyl azide) and a terminal alkyne, leading to a cuprated ketenimine intermediate prone to be trapped by a water nucleophile is summarized in Scheme 4.

Scheme 4. Catalytic cycle derived from DFT calculation

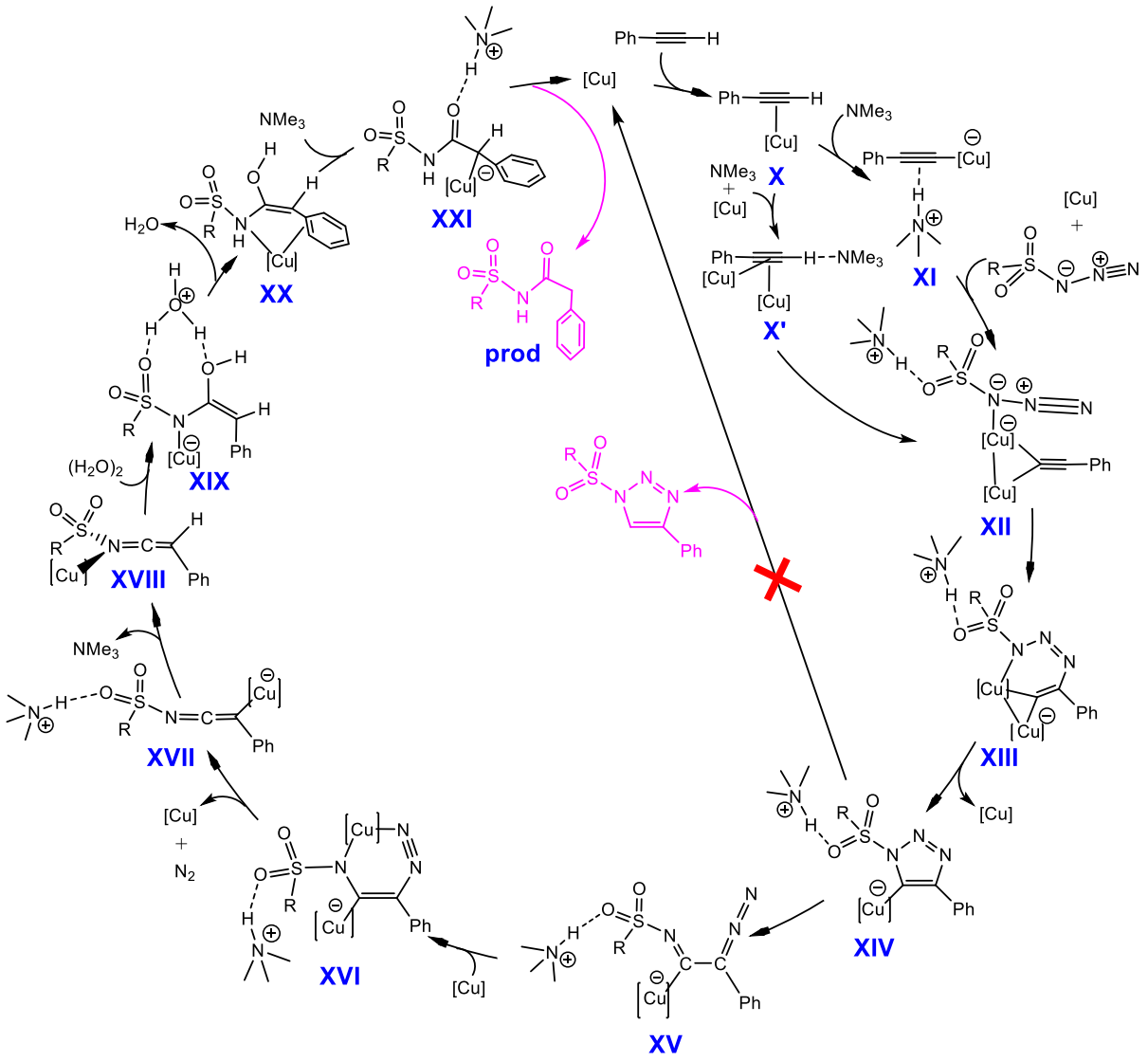

The catalytic cycle is initiated by coordination of a terminal alkyne to a Cu complex, acidifying the alkyne hydrogen and making it labile to be deprotonated by a mild base like an amine to give **XI**. The resultant σ-acetylide complex is a highly efficient scavenger of a second Cu complex which gives **XII** in the presence of mesyl azide. A competitive alternative for formation of key intermediate **XII** is coordination of the Cu complex to **X** followed by deprotonation and then coordination of mesyl azide (intermediacy of **X′**). This dicuprated complex is reactive toward cyclisation to yield **XIV**, preceded by the release of the second Cu complex from **XIII**. Complex **XIV** is a branching point for two competitive pathways (i) protodecupration (ii) ring opening/N_2 elimination. We found that the latter is more favourable if it involves a second Cu for the N_2 elimination step i.e. transformation **XV → XVI → XVII**. For cuprated ketenimine **XVII** to react with water as a nucleophile, it first needs to undergo protodecupration to give intermediate **XVIII**. Coordination of a Cu complex to the nitrogen atom in this intermediate activates the ketenimine toward nucleophilic attack by water to afford

XIX. The oxygen bonded hydrogen in intermediate **XX** is so acidic that it can be deprotonated by a base results in intermediate **XXI**. Finally the catalytic cycle is complete through protodecupration which converts **XXI** to **prod**.

CONCLUSION

DFT calculations were used to study the Cu(I)-catalysed click reaction involving a ketenimine as the key intermediate in reaction with nucleophilic water. Our results provide a better understanding of the copper-catalysed click reaction mechanism, a rationale for the effects of the azide nature on the reaction mechanism, and an explanation for why one pathway is preferred over another. Several points have emerged from our investigation:

(1) It is well established that in this class of catalysis, a cuprated triazole intermediate (**A** in Table 1) is formed whose stability against N_2 elimination is determined by the nature of its R substituent. We found that the stability of cuprated triazoles is sensitive to the nature of the N-N bond being cleaved. Electron withdrawing R substituents reduce the strength of the N-N bond, thus facilitating the N_2 elimination.

(2) The cycloaddition step of these catalytic reactions is postulated to proceed through a binuclear mechanism. We found that the binuclear mechanism is preferred because once the copper(I) acetylide intermediate (**11** in Figure 3) is formed, it operates as an efficient copper(I) scavenger. Formation of the binuclear Cu complex further stabilises the system, making the cycloaddition step accessible with a much lower activation barrier.

(3) The cuprated triazole intermediate is a branching point for two competitive pathways: (i) protodecupration and (ii) ring opening/N_2 elimination (Figure 4). We conclude from our calculations that, for the mesyl azide model substrate, the N_2 elimination step is accelerated if it involves a second copper complex. In the absence of the second copper complex, protodecupration is calculated to have a lower activation barrier than N_2 elimination. This is in disagreement experimental findings for which the protodecupration product is rarely reported.

(4) When the ring opening/N_2 elimination step is complete, a ketenimine intermediate is produced (**23** in Figure 7). This intermediate reacts easily with water only if it is activated by a Cu complex coordinating to its nitrogen. We discovered that the cuprated ketenimine intermediate itself (**19** in Figure 7) is unlikely to be directly involved in a hydrolysis process.

COMPUTATIONAL DETAILS

Gaussian 09 [16] was used to fully optimize all the structures reported in this paper at the B3LYP level of density functional theory (DFT)[17] in chloroform using the CPCM[18] solvation model. The effective-core potential of Hay and Wadt with a double-ξ valence basis set (LANL2DZ)[19] was chosen to describe Cu and I. The 6-31G(d) basis set was used for other atoms.[20] Polarization functions were also added for Cu (ξ_f =3.525) and I (ξ_f = 0.289).[21] This basis set combination will be referred to as BS1. Frequency calculations were carried out at the same level of theory as those for the structural optimization. Transition structures were located using the Berny algorithm. Intrinsic reaction coordinate (IRC)[22] calculations were used to confirm the connectivity between transition structures and minima. To further refine the energies obtained from the B3LYP/BS1 calculations, we carried out single-point energy calculations for all of the structures with a larger basis set (BS2) in chloroform using the CPCM solvation model. BS2 utilizes the def2-TZVP basis set[23] on all atoms. An effective core potential including scalar relativistic effect was used for iodine atom. The B3LYP-D3BJ[24] calculations were used to overcome the deficiency of the B3LYP level in incorporating long-range correlation for dispersion forces. To estimate the corresponding enthalpy, ΔH, and Gibbs energies, ΔG, the corrections were calculated at the B3LYP/BS1 level and finally added to the single-point energies. The potential and Gibbs free energies obtained from the B3LYP-D3BJ/BS2//B3LYP/BS1 calculations in chloroform are used for interpreting the obtained results.

To investigate how sensitive the relative energies are to the nature of the employed basis sets, we replaced BS2 with BS3; the latter uses def2-QZVP for the Cu and I atoms and 6-311+G(2d,p) for other atoms; an effective core potential including scalar relativistic effect was used for iodine atom. We found that basis set dependence for such a system is not very significant. For example, using the B3LYP-D3BJ-CPCM/BS2//B3LYP-CPCM/BS1 level, the relative Gibbs energies of $\mathbf{TS_{A\text{-}B}}$, **B**, and $\mathbf{TS_{B\text{-}C}}$ where R = CH_3SO_2 (Table 1) are calculated to be 12.9, 9.3, and 17.3 kcal/mol, respectively, while using the B3LYP-D3BJ-CPCM/BS3//B3LYP-CPCM/BS1 level, those are calculated to be 13.2, 9.4, and 17.3 kcal/mol, respectively.

ASSOCIATED CONTENT

Supporting Information

The Supporting Information is available free of charge on the ACS Publications website.

Figures S1-S5 and Table S1 (PDF)

Cartesian coordintes of all calculated species (XYZ)

AUTHOR INFORMATION

Corresponding Author

*E-mail for A.A.: alirezaa@utas.edu.au.

ORCID

Alireza Ariafard: 0000-0003-2383-6380

Notes

The authors declare no competing financial interest.

ACKNOWLEDGMENT

The authors gratefully acknowledge the generous allocation of computing time from Australian National Computational Infrastructure and University of Tasmania. A. A., B. F. Y., and A. C. also thanks the Australian Research Council for financial support (project number DP180100904).

REFERENCES

[1] (a) Himo, F.; Lovell, T.; Hilgraf, R.; Rostovtsev, V. V.; Noodleman, L.; Sharpless, K. B.; Fokin, V. V. Copper(I)-catalyzed synthesis of azoles. DFT study predicts unprecedented reactivity and intermediates. *J. Am. Chem. Soc.* **2005**, *127*, 210-216. (b) Bock, V. D.; Hiemstra, H.; van Maarseveen, J. H. Cu^{I}-Catalyzed Alkyne–Azide "Click" Cycloadditions from a Mechanistic and Synthetic Perspective. *Eur. J. Org. Chem.* **2006**, *1*, 51-68. (c) Meldal, M.; Tornoe, C. W. Cu-catalyzed azide-alkyne cycloaddition. *Chem. Rev.* **2008**, *108*, 2952-3015. (d) Hein, J. E.; Fokin, V. V. Copper-catalyzed azide-alkyne cycloaddition (CuAAC) and beyond: new reactivity of copper(I) acetylides. *Chem. Soc. Rev.* **2010**, *39*, 1302-1315. (e) Kim, S. H.; Park, S. H.; Choi, J. H.; Chang, S. Sulfonyl and Phosphoryl Azides: Going Further Beyond the Click Realm of Alkyl and Aryl Azides. *Chemistry–An Asian Journal* **2011,** *6*, 2618-2634. (f) Berg, R.; Straub, B. F. Advancements in the mechanistic understanding of the copper-catalyzed azide-alkyne cycloaddition. *Beilstein J. Org. Chem*. **2013**, *9*, 2715-2750. (g) Madhu, N.; Namitharan, K. Copper-Catalyzed Sulfonyl Azide–Alkyne Cycloaddition Reactions: Simultaneous Generation and Trapping of Copper Triazoles and −Ketenimines for the Synthesis of Triazolopyrimidines. *Org. Lett.* **2017,** *13*, 3536-3539.

[2] (a) Wu, P.; Feldman, A. K.; Nugent, A. K.; Hawker, C. J.; Scheel, A.; Voit, B.; Pyun, J.; Frechet, J. M. J.; Sharpless, K. B.; Fokin, V. V. Efficiency and fidelity in a click-chemistry route to triazole dendrimers by the copper(i)-catalyzed ligation of azides and alkynes. *Angew. Chem. Int. Ed*. **2004**, *116*, 4018-4022. (b) Wu, P.; Malkoch, M.; Hunt, J. N.; Vestberg, R.; Kaltgrad, E.; Finn, M. G.; Fokin, V. V.; Sharpless, K. B.; Hawker, C. Multivalent, bifunctional dendrimers prepared by click chemistry. *J. Chem. Commun*. **2005**, *46*, 5775-5777. (c) Laurent, B. A.; Grayson, S. M. An efficient route to well-defined macrocyclic polymers via "click" cyclization. *J. Am. Chem. Soc*. **2006**, *128*, 4238-4239. (d) Moses, J. E.; Moorhouse, A. D. The

growing applications of click chemistry. *Chem. Soc. Rev.* **2007**, *36*, 1249-1262. (e) Amélie, N.; Tilley, T. D. Selective Synthesis of a Series of Isostructural MIICuI Heterobimetallic Complexes Spontaneously Assembled by an Unsymmetrical Naphthyridine-Based Ligand. *Chem. Eur. J.* **2018,** *24*, 10329-10333.

[3] (a) Wang, Q.; Chan, T. R.; Hilgraf, R.; Fokin, V. V.; Sharpless, K. B.; Finn, M. G. Bioconjugation by copper(I)-catalyzed azide-alkyne [3 + 2] cycloaddition. *J. Am. Chem. Soc.* **2003**, *125*, 3192-3193. (b) Xue-Long, S.; Stabler, C. L.; Cazalis, C. S.; Chaikof, E. L. Carbohydrate and protein immobilization onto solid surfaces by sequential diels− alder and azide− alkyne cycloadditions. *Bioconjugate chem.* **2006,** *17*, 52-57. (c) Tiwari, V. K.; Mishra, B. B.; Mishra, K. B.; Mishra, N.; Singh, A. S.; Chen, X. Cu-Catalyzed Click Reaction in Carbohydrate Chemistry. *Chem. rev.* **2016**, *116*, 3086-3240. (d) Li, L.; Zhang, Z. Development and Applications of the Copper-Catalyzed Azide-Alkyne Cycloaddition (CuAAC) as a Bioorthogonal Reaction. *Molecules* **2016**, *21,* 1393.

[4] (a) Kolb, H. C.; Finn, M. G.; Sharpless, K. B. Click Chemistry: Diverse Chemical Function from a Few Good Reactions. *Angew. Chem. Int. Ed*. **2001**, *40*, 2004-2021. (b) Tornøe, C. W.; Christensen, C.; Meldal, M. Peptidotriazoles on Solid Phase: [1,2,3]-Triazoles by Regiospecific Copper(I)-Catalyzed 1,3 Dipolar Cycloadditions of Terminal Alkynes to Azides. *J. Org. Chem*. **2002**, *67*, 3057-3064. (c) Rostovtsev, V. V.; Green, L. G.; Fokin, V. V.; Sharpless, K. B. A Stepwise Huisgen Cycloaddition Process: Copper(I)-Catalyzed Regioselective "Ligation" of Azides and Terminal Alkynes*. *Angew. Chem. Int. Ed*. **2002**, *114*, 2708-2711. (d) Lewis, W. G.; Green, L. G.; Grynszpan, F.; Radic, Z.; Carlier, P. R.; Taylor, P.; Finn, M. G.; Sharpless, K. B. Click chemistry in situ: acetylcholinesterase as a reaction vessel for the selective assembly of a femtomolar inhibitor from an array of building blocks. *Angew. Chem.* **2002**, *114*, 1095-1099. (e) Kolb, H. C.; Sharpless, K. B. The growing impact of click chemistry on drug discovery. *Drug Discovery Today* **2003**, *8*, 1128-1137. (f) Moorhouse, A. D.; Santos, A. M.; Gunaratnam, M.; Moore, M.; Neidle, S.; Moses, J. E. Stabilization of G-quadruplex DNA by highly selective ligands via click chemistry. *J. Am.Chem. Soc.* **2006**, *128*, 15972-15973.

[5] a) Ahlquist, M.; Fokin, V.V. Enhanced reactivity of dinuclear copper (I) acetylides in dipolar cycloadditions. *Organometallics,* **2005,** *26*, 4389-4391. b) Straub, B.F. μ-Acetylide and μ-alkenylidene ligands in "click" triazole syntheses. *J. Chem. Commun.* **2007,** 37, 3868-3870.

[6] Bae, I.; Han, H.; Chang, S. Highly efficient one-pot synthesis of N-sulfonylamidines by Cu-catalyzed three-component coupling of sulfonyl azide, alkyne, and amine. *J. Am. Chem. Soc.* **2005**, 127, 2038-2039.

[7] (a) Rodionov, V. O.; Fokin, V. V.; Finn, M. G. Mechanism of the ligand-free CuI-catalyzed azide-alkyne cycloaddition reaction. *Angew. Chem.* ***2005,*** *117*, 2250-2255; *Angew. Chem. Int. Ed*. **2005**, *44*, 2210-2215. (b) Worrell, B. T.; Malik, J. A.; Fokin, V. V. Direct evidence of a dinuclear copper intermediate in Cu(I)-catalyzed azide-alkyne cycloadditions. *Science* **2013,** *340*, 457-460.

[8] (a) Buckley, B.; Sandra, E. D.; Heaney, H. Experimental evidence for the involvement of dinuclear alkynylcopper (I) complexes in alkyne–azide chemistry. *Chem. Eur. J.* **2010**, *16*, 6278-6284. (b) Presolski, S. I.; Hong, V.; Cho, S. H.; Finn, M. G. Tailored ligand acceleration of the Cu-catalyzed azide-alkyne cycloaddition reaction: practical and mechanistic implications. *J. Am. Chem. Soc*. **2010**, *132*, 14570-14576. (c) Cantillo, D.; Ávalos, M.; Babiano, R.; Cintas, P.; Jiménez, J. J. L.; Palacios, J. C. Assessing the whole range of CuAAC mechanisms by DFT calculations--on the intermediacy of copper acetylides. *Org. Biomol.*

Chem. **2011**, *9*, 2952-2958. (d) Kuang, G.; Guha, P. M.; Brotherton, W. S.; Simmons, J. T.; Stankee, L. A.; Nguyen, B. T.; Clark, R. J.; Zhu, L. Experimental investigation on the mechanism of chelation-assisted, copper(II) acetate-accelerated azide-alkyne cycloaddition. *J. Am. Chem. Soc.* **2011**, *133*, 13984-14001. (e) Iacobucci, C.; Reale, S.; Gal, J. F.; de Angelis, F. Dinuclear copper intermediates in copper(I)-catalyzed azide-alkyne cycloaddition directly observed by electrospray ionization mass spectrometry. *Angew. Chem. Int. Ed.* **2015**, *54*, 3065-3068. (f) Özkılıç, Y.; Tüzün, N. Ş. A DFT Study on the Binuclear CuAAC Reaction: Mechanism in Light of New Experiments. *Organometallics* **2016**, *35*, 2589-2599. (g) Wang, C.; Ikhlef, D.; Kahlal, S.; Saillard, J. Y.; Astruc, D. Metal-catalyzed azide-alkyne "click" reactions: Mechanistic overview and recent trends. *Coordination Chemistry Reviews* **2016**, *316*, 1-20. (h) Chen, H.; Cai, C.; Li, S.; Ma, Y.; Luozhong, S.; Zhu, Z. Intermediates Stabilized by Tris(triazolylmethyl)amines in the CuAAC Reaction. *Chem. Eur. J.* **2017**, *23*, 4730-4735.

[9] Chauhan, D. P.; Varma, S. J.; Vijeta, A.; Banerjee, P.; Talukdar, P. A 1,3-amino group migration route to form acrylamidines. *Chem. Commun.* **2014**, *50*, 323-325.

[10] Wang, J.; Lu, P.; Wang, Y. Copper-catalyzed multi-component synthesis of acrylamidines and benzoimidazoles. *Org. Chem. Front.* **2015**, *2*, 1346-1351.

[11] (a) Yoo, E. J.; Ahlquist, M.; Kim, S. H.; Bae, I.; Fokin, V. V.; Sharpless, K. B.; Chang, S. Copper-catalyzed synthesis of N-sulfonyl-1,2,3-triazoles: controlling selectivity. *Angew. Chem. Int. Ed.* **2007**, *46*, 1730-1733; *Angew. Chem.* **2007**, *119*, 1760-1763. (b) Yoo, E. J.; Ahlquist, M.; Bae, I.; Sharpless, K. B.; Fokin, V. V.; Chang, S. Mechanistic studies on the Cu-catalyzed three-component reactions of sulfonyl azides, 1-alkynes and amines, alcohols, or water: dichotomy via a common pathway. *J. Org. Chem.* **2008,** *73*, 5520-5528. (c) Cassidy, M. P.; Raushel, J.; Fokin, V.V. Practical Synthesis of Amides from In Situ Generated Copper(I) Acetylides and Sulfonyl Azides. *Angew. Chem.* **2006**, *118*, 3226-3229.

[12] Haldon, E.; Nicasio, M. C.; Perez, P. J. Copper-catalysed azide-alkyne cycloadditions (CuAAC): an update. *Org. Biomol. Chem.* **2015,** *13*, 9528-9550.

[13] Cho, S. H.; Yoo, E. J.; Bae, I.; Chang, S. Copper-catalyzed hydrative amide synthesis with terminal alkyne, sulfonyl azide, and water. *J. Am. Chem. Soc.* **2005,** *127*, 16046-16047.

[14] The charge separation process was also tested for other outer-sphere complexes; for example, this process starting from complexes **13** and **19** is calculated to be endergonic about 17.9 and 22.1 kcal/mol, respectively. It follows from these results that the NMe_3H^+ cation prefers to remain in proximity to an anionic copper complex during the catalytic reaction.

[15] Formation of a geminally dicuprated acetylide complex was also shown by Himo et al. that plays an important role in facilitating catalytic kinugasa reaction. For details, see: Santoro, S.; Liao, R. Z.; Marcelli, T.; Hammar, P.; Himo, F. Theoretical Study of Mechanism and Stereoselectivity of Catalytic Kinugasa Reaction. *J. Org. Chem.* **2015**, 80, 2649−2660.

[16] Frisch, M. J.; Trucks, G. W.; Schlegel, H. B.; Scuseria, G. E.; Robb, M. A.; Cheeseman, J. R.; Scalmani, G.; Barone, V.; Mennucci, B.; Petersson, G. A.; Nakatsuji, H.; Caricato, M.; Li, X.; Hratchian, H. P.; Izmaylov, A. F.; Bloino, J.; Zheng, G.; Sonnenberg, J. L.; Hada, M.; Ehara, M.; Toyota, K.; Fukuda, R.; Hasegawa, J.; Ishida, M.; Nakajima, T.; Honda, Y.; Kitao, O.; Nakai, H.; Vreven, T.; Montgomery, J. A.; Peralta, Jr., J. E.; Ogliaro, F.; Bearpark, M.; Heyd, J. J.; Brothers, E.; Kudin, K. N.; Staroverov, V. N.; Kobayashi, R.; Normand, J.;

Raghavachari, K.; Rendell, A.; Burant, J. C.; Iyengar, S. S.; Tomasi, J.; Cossi, M.; Rega, N.; Millam, J. M.; Klene, M.; Knox, J. E.; Cross, J. B.; Bakken, V.; Adamo, C.; Jaramillo, J.; Gomperts, R.; Stratmann, R. E.; Yazyev, O.; Austin, A. J.; Cammi, R.; Pomelli, C.; Ochterski, J. W.; Martin, R. L.; Morokuma, K.; Zakrzewski, V. G.; Voth, G. A.; Salvador, P.; Dannenberg, J. J.; Dapprich, S.; Daniels, A. D.; Farkas, O.; Foresman, J. B.; Ortiz, J. V.; Cioslowski, J.; Fox, D. J. Gaussian 09, Revision D.01; Gaussian, Inc.: Wallingford, CT, **2009**.

[17] (a) Zhao, Y.; Schultz, N. E.; Truhlar, D. G. Design of density functionals by combining the method of constraint satisfaction with parametrization for thermochemistry, thermochemical kinetics, and noncovalent interactions. *J. Chem. Theory Comput.* **2006**, *2*, 364-382. (b) Zhao, Y.; Truhlar, D. G. A new local density functional for main-group thermochemistry, transition metal bonding, thermochemical kinetics, and noncovalent interactions. *J. Chem. Phys.* **2006**, *125*, 194101. (c) Zhao, Y.; Truhlar, D. G. Density Functional for Spectroscopy: No Long-Range Self-Interaction Error, Good Performance for Rydberg and Charge-Transfer States, and Better Performance on Average than B3LYP for Ground States. *J. Phys. Chem. A*. **2006**, *110*, 13126-13130.

[18] Barone, V.; Cossi, M. Quantum Calculation of Molecular Energies and Energy Gradients in Solution by a Conductor Solvent Model. *J. Phys. Chem. A.* **1998**, *102*, 1995-2001.

[19] (a) Hay, P. J.; Wadt, W. R. Ab initio effective core potentials for molecular calculations. Potentials for the transition metal atoms Sc to Hg. *J. Chem. Phys.* **1985**, *82*, 270-283. (b) Wadt, W. R.; Hay, P. Ab initio effective core potentials for molecular calculations. Potentials for main group elements Na to Bi. *J. Chem. Phys*. **1985**, *82*, 284-298.

[20] Hariharan, P. C.; Pople, J. A. The influence of polarization functions on molecular orbital hydrogenation energies. *Theor. Chim. Acta.* **1973**, *28*, 213-222.

[21] (a) Ehlers, A. W.; Böhme, M.; Dapprich, S.; Gobbi, A.; Höllwarth, A.; Jonas, V.; Köhler, K. F.; Stegmann, R.; Veldkamp, A.; Frenking, G. A set of f-polarization functions for pseudo-potential basis sets of the transition metals ScCu, YAg and LaAu. *Chem. Phys. Lett.* **1993**, *208*, 111-114. (b) Höllwarth, A.; Böhme, M.; Dapprich, S.; Ehlers, A. W.; Gobbi, A.; Jonas, V.; Köhler, K. F.; Stegmenn, R.; Veldkamp, A.; Frenking, G. A set of d-polarization functions for pseudo-potential basis sets of the main group elements Al-Bi and f-type polarization functions for Zn, Cd, Hg. *Chem. Phys. Lett*. **1993**, *208*, 237-240.

[22] (a) Fukui, K. Formulation of the reaction coordinate. *J. Phys. Chem*. **1970**, *74*, 4161-4163. (b) Fukui, K. The path of chemical reactions - the IRC approach. *Acc. Chem. Res*. **1981**, *14*, 363-368.

[23] Weigend, F.; Furche, F.; Ahlrichs, R. Gaussian basis sets of quadruple zeta valence quality for atoms H–Kr. *J. Chem. Phys.* **2003**, *119*, 12753-12762.

[24] Grimme, S.; Antony, J.; Ehrlich, S.; Krieg, H. A consistent and accurate ab initio parametrization of density functional dispersion correction (DFT-D) for the 94 elements H-Pu. *J. Chem. Phys*. **2010**, *132*, 154104-154122.